

FANO RESONANCES IN A BILAYER STRUCTURE COMPOSED OF TWO KINDS OF DISPERSIVE META-MATERIALS

Y. Liu^{1,2}, H. Jiang^{1,*}, C. Xue¹, W. Tan¹, H. Chen¹, and Y. Shi^{1,2}

¹Key Laboratory of Advanced Micro-structure Materials, MOE, Department of Physics, Tongji University, Shanghai 200092, China

²Institute of Solid State Physics, Shanxi Datong University, Datong 037009, China

Abstract—We theoretically find that a bi-layer structure composed of two kinds of dispersive metamaterials can possess an asymmetric reflection spectrum due to Fano-type interference between a discrete reflection resonance and a broadband strong reflection. The discrete reflection resonance appears at the frequency around which the dispersive permeability is near to zero at oblique incidence. Based on analytical and numerical analysis, the asymmetric factor in the Fano-type reflection is found to be linked with the angle of incidence.

1. INTRODUCTION

Fano resonance attracts interest due to its universality in many physical systems. The shape of the Fano resonance [1] that is distinct from that of conventional symmetric resonance curves arises from the constructive and destructive interference of a narrow discrete resonance with a broad spectral line or continuum. In his original paper, Fano derived a simple expression:

$$F(\Omega) = \frac{(\Omega + q)^2}{\Omega^2 + 1}, \quad (1)$$

where Ω is the dimensionless frequency defined by the central frequency and the width of the autoionizing state, and q is the Fano asymmetry parameter, a ratio of the transition probabilities to the mixed state and to the continuum [2], which describes the degree of asymmetry.

Received 22 July 2011, Accepted 17 August 2011, Scheduled 19 August 2011

* Corresponding author: Haitao Jiang (jiang-haitao@tongji.edu.cn).

After Fano resonance was discovered in the atomic system, Fano-type asymmetric line shapes have been observed in many other systems [3–15]. In particular, Fano resonances realized in classical systems deserve special attention. In 2002, Fan found that asymmetric Fano resonance can occur in a two-dimensional photonic-crystal waveguide side coupled with a microcavity [6]. After that, many kinds of Fano-type resonances were found in various kinds of photonic-crystal systems [7–10]. For example, Rybin et al. found that Fano resonance can be realized in a three-dimensional (3D) photonic crystal with defects due to Mie and Bragg scatterings [11]. Moreover, Fano resonances have been observed in a number of nanoscale systems including plasmonic nanostructures [12] or metamaterials [13,14]. For instance, in periodic metallic structures or asymmetric slits in a metallic film, Fano resonances widely exist. Metamaterials composed of resonant unit cells can also possess many kinds of Fano resonances. In the analogy of electromagnetic-induced transparency in metamaterials, Fano resonance occurs due to the interference between two non-degenerated modes split by symmetry broken. If chirality is introduced into 3D metamaterials, double Fano resonances can appear, which can be used for realizing broadband slow waves [15].

In this paper, we study another type of Fano resonance in metamaterials. We concentrate on single-negative (SNG) metamaterials including ε -negative (ENG) material ($\varepsilon < 0, \mu > 0$) [16] and μ -negative (MNG) material ($\varepsilon > 0, \mu < 0$) [17]. In the optical frequency range, metal works as a natural ENG material below plasma frequency [18]. The MNG material need be achieved in a planar structure composed of nonmagnetic conductive resonant elements [19]. A single ENG or MNG layer is opaque for electromagnetic (EM) waves since the wavevectors are complex. However, in 2003 Alù and Engheta found that EM waves can resonantly tunnel through an ENG/MNG bilayer under impedance and phase matching conditions [20]. The dependence of resonant tunneling on static positive parameters has been discussed in detail recently [21]. In 2007, Alù et al. discovered that an EM wave with transverse magnetic (TM) [transverse electric (TE)] polarization cannot transport through a single zero-permittivity (permeability) slab, unless the impinging plane wave comes exactly at normal incidence [22]. In this paper, we study an ENG/MNG bilayer in which the MNG layer can approach zero permeability at some frequency and lead to an asymmetric Fano-type resonances. The paper is organized as follows. In Section 2, we analytically and numerically discuss the physical mechanism of this type of Fano resonance in detail. In particular, we study the dependence of the Fano shape on the angle of incidence. Finally we conclude in Section 3.

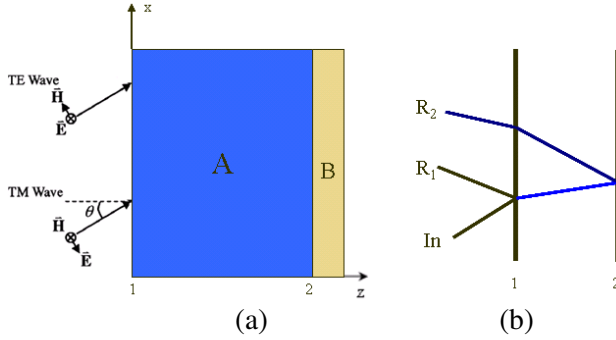


Figure 1. Prototype system for the Fano resonance. (a) Scheme for ENG/MNG bilayer structure. (b) The two possible reflection pathways, namely, reflection R1 at surface 1 and reflection R2 at the interface 2.

2. ASYMMETRIC REFLECTION SPECTRUM

Figure 1(a) illustrates the scheme of an ENG/MNG bilayer for Fano-like resonance, in TE and TM polarization case. Figure 1(b) shows that there are two possible reflection pathways. One reflection pathway is the broadband reflection R1 at the entrance face of the ENG layer (denoted by A) that is the background reflection, and the other is the narrow reflection R2 occurring at the entrance face of the MNG layer (denoted by B) with nearly zero permeability. In the following calculations, we only consider TE polarization. For TM polarization, we only need to change A (B) into a MNG (ENG) layer according to the duality principle. We supposed that ENG layer has a relative dielectric permittivity ϵ_{ENG} , relative magnetic permeability μ_{ENG} and a thickness of a nm and MNG layer has a relative magnetic permeability μ_{MNG} , relative dielectric permittivity ϵ_{MNG} and a thickness of b nm. We choose a Drude-like response for the dielectric permittivity of the ENG layer and magnetic permeability of MNG layer,

$$\begin{aligned} \epsilon_{ENG} &= \epsilon - \frac{\omega_e^2}{\omega(\omega + i\gamma_e)} \\ \mu_{MNG} &= \mu - \frac{\omega_m^2}{\omega(\omega - i\gamma_m)}, \end{aligned} \tag{2}$$

where ω_e and ω_m denotes the electronic and magnetic plasma frequencies, respectively, and γ denotes the damping.

By means of the transfer-matrix method [23], we calculate the reflection spectrum of the monolayer SNG material. In the following

calculation, we choose $\varepsilon = 0.4$, $\mu = 1$, $\varepsilon_{MNG} = \mu_{ENG} = 1$, $\omega_e = \omega_m = 2\pi \times 300$ THz and $\gamma = \omega_e(\omega_m) \times 10^{-3}$ THz. Around the frequency of plasmon ($f = \omega_m/2\pi = 300$ THz), the dispersive permeability of the MNG is near to zero ($\mu_{MNG} \rightarrow 0$). The angle of incidence is selected to be $\pi/18$, $2\pi/9$ and $4\pi/9$, respectively. Fig. 2(a) shows the broadband reflection spectra of the ENG layer. Because the ENG materials are opaque, the reflection of light at its surface can be treated as a strong reflection continuum. Fig. 2(b) gives the reflection spectrum of the MNG layer at oblique incidence. It is shown that there is no reflection at normal incidence [22]. However, at oblique incidence, a reflection peak is excited at the plasma frequency due to the total internal reflection at the surface of MNG layer (strong impedance mismatch). Moreover, the quality factor of the reflection resonance decreases with the increase of incident angle, as seen by Fig. 2(b).

For the ENG/MNG bilayer, when the light impinges on the structure at oblique incidence, it can be reflected partially on the entrance of ENG layer, forming the strong reflection continuum. Meanwhile, the optical wave penetrating through ENG slab will be reflected by the MNG layer, and a narrow discrete reflection resonance will appear when the permeability of MNG approaches to zero. We choose $a = 120$ nm and $b = 10$ nm. If the loss of the MNG is small, the frequency satisfying $\mu_{MNG} \rightarrow 0$ is $f = \omega_m/2\pi = 300$ THz.

At first, we derive the analytical expression of the reflectance of the ENG/MNG bilayer. For the TE case, by means of the transfer-matrix method, one can obtain the reflection coefficient:

$$r = \frac{\left(m_{11} + m_{12} \frac{k_{0z}}{k_0}\right) - \frac{k_0}{k_{0z}} \left(m_{21} + m_{22} \frac{k_{0z}}{k_0}\right)}{\left(m_{11} + m_{12} \frac{k_{0z}}{k_0}\right) + \frac{k_0}{k_{0z}} \left(m_{21} + m_{22} \frac{k_{0z}}{k_0}\right)}, \quad (3)$$

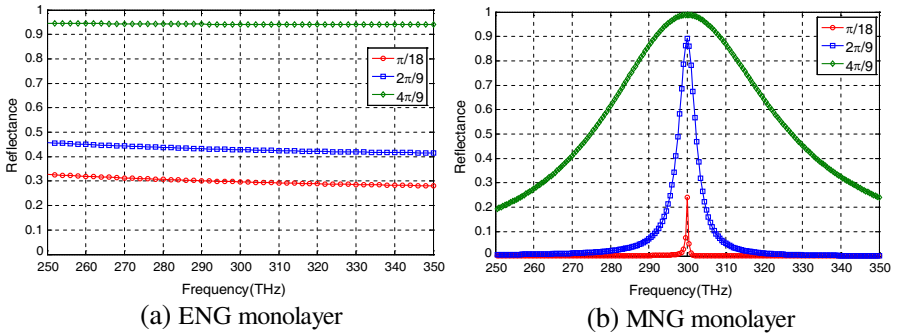


Figure 2. The broadband reflection spectra of the ENG layer (a) and the discrete reflection resonance of the dispersive MNG layer (b) for TE modes. The angle of incident is $\pi/18$, $2\pi/9$ and $4\pi/9$, respectively.

where $m_{i,j}$ ($i, j = 1, 2$) is the matrix elements of

$$M = \prod_{j=1}^2 M_j = \prod_{j=1}^2 \begin{pmatrix} \cos(k_{jz}d_j) & -\frac{ik_{jz}}{k_0\mu_j} \sin(k_{jz}d_j) \\ -i\frac{k_0\mu_j}{k_{jz}} \sin(k_{jz}d_j) & \cos(k_{jz}d_j) \end{pmatrix} = \begin{pmatrix} m_{11} & m_{12} \\ m_{21} & m_{22} \end{pmatrix}, \tag{4}$$

in which $k_{jz} = \sqrt{k_j^2 - \beta^2}$ is the z component of wave vector in the j th layer; $k_0 = \omega\sqrt{\varepsilon_0\mu_0}$ represents the wave number in free space; $\beta = k_0 \cos \theta$ is the parallel wave vector.

In detail, the matrix elements can be written as:

$$\begin{aligned} m_{11} &= \cos(k_{Az}a) \cos(k_{Bz}b) - \frac{\mu_B k_{Az}}{\mu_A k_{Bz}} \sin(k_{Az}a) \sin(k_{Bz}b) \\ m_{12} &= -\frac{ik_{Bz}}{k_0\mu_B} \cos(k_{Az}a) \sin(k_{Bz}b) - \frac{ik_{Az}}{k_0\mu_A} \cos(k_{Bz}b) \sin(k_{Az}a) \\ m_{21} &= -\frac{k_0\mu_A}{k_{Az}} \cos(k_{Bz}b) \sin(k_{Az}a) - \frac{k_0\mu_B}{k_{Bz}} \cos(k_{Az}a) \sin(k_{Bz}b) \\ m_{22} &= -\frac{\mu_A k_{Bz}}{\mu_B k_{Az}} \sin(k_{Az}a) \sin(k_{Bz}b) + \cos(k_{Az}a) \cos(k_{Bz}b) \end{aligned} \tag{5}$$

Because the thickness of each layer is much smaller than the wavelength, we have $|k_{jz}|d_j \ll 1$ ($j = 1, 2$), i.e., $|k_{Az}|a \ll 1$, $|k_{Bz}|b \ll 1$, where $|k_{jz}|$ is the module of the complex k_{jz} . For small losses in Eq. (2), k_{jz} can be approximated to a pure imaginary number. As a result, $\cos(k_{jz}d_j)$ and $\sin(k_{jz}d_j)$ can be written as $\cosh(|k_{jz}|d_j)$ and $\sinh(|k_{jz}|d_j)$, respectively, and one can expand $\cosh(|k_{jz}|d_j)$ and $\sinh(|k_{jz}|d_j)$ in a Taylor series,

$$\begin{aligned} \cosh(|k_{jz}|d_j) &= 1 + \frac{(|k_{jz}|d_j)^2}{2} + O\left((|k_{jz}|d_j)^4\right), \\ \sinh(|k_{jz}|d_j) &= |k_{jz}|d_j + O\left((|k_{jz}|d_j)^3\right). \end{aligned} \tag{6}$$

Then, we neglect the high-order terms in the Taylor expansion of Eq. (6) and substitute the simplified Eq. (6) into Eq. (5). Assuming the permittivity of the ENG, $\varepsilon_A = -\alpha$ ($\alpha > 0$), when the permeability of the MNG layer is near zero, in the subwavelength limit Eq. (3) can be eventually written as:

$$r(\beta) \stackrel{\mu_B \rightarrow 0}{\approx} \frac{-k_0^2 a + i [b - a(\alpha + \beta^2)] \left[1 - \left(\frac{\beta}{k_0}\right)^2 \right]}{k_0^2 a + 2k_0 \left[1 - \left(\frac{\beta}{k_0}\right)^2 \right]^{1/2} + i [b - a(\alpha + \beta^2)] \left[1 - \left(\frac{\beta}{k_0}\right)^2 \right]}. \tag{7}$$

As a result, we can calculate the reflectance R and it may be understood within Fano scattering framework, in which an asymmetric

profile in the spectrum can follow the profile:

$$R(\beta) = r^* \cdot r = \frac{1}{1 + \zeta(\beta)^2} \frac{[\Omega(\omega, \beta) + \zeta(\beta)]^2}{\Omega(\omega, \beta)^2 + 1}. \quad (8)$$

In Eq. (8), $\zeta(\beta) = k_0^4/(k_0^2 - \beta^2)$ corresponds to the Fano asymmetry parameter q and it increases with β . $\Omega(\omega, \beta)$ is a function of frequency and β . In Fig. 3, the top and bottom graphs numerically show the variances of Fano-like reflection and transmission spectra with different incident angles, i.e., different values of β , respectively, by means of the transfer-matrix method. As expected by the analytical model of Eq. (8), the reflection spectrum strongly depends on the β parameter. With the increase of β parameter, we obtained good fitting of the spectra by calculations of Eq. (8). This result confirms that Fano-like interference between the broadband strong reflection spectrum and discrete reflection peak occurs. Moreover, during the fitting procedure, we find that the Fano asymmetry parameter is changing continuously with the increase of the incident angle in the studied range from $\pi/18$ to $4\pi/9$. The Fano parameter q increases with the β parameter. And the asymmetry reflectance is similar to the schematics of the possible Fano resonance in Ref. [7]. As seen from Figs. 3(a)–(b), we can conclude that the asymmetry reflection peak transforms into the symmetry reflection dip with the increase of the Fano parameter. The corresponding Fano-like transmission spectra are also shown in Figs. 3(a')–3(c'). Finally, in Fig. 4 we calculate the distributions of the intensity of fields at the frequency near the reflected valley in Fig. 3(a) (299.5 THz). The intensity of the incident fields is supposed to be 1. From Fig. 4, we can find what is remarkable here is that the amplitude of the local magnetic

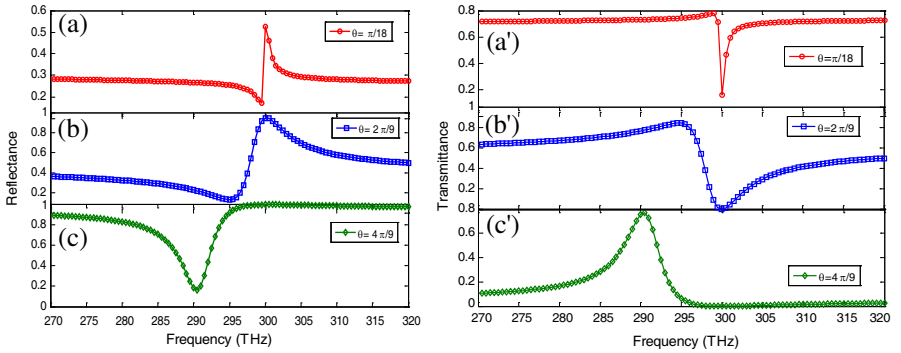


Figure 3. The variances of the reflectance [(a), (b) and (c)] and transmittance [(a'), (b') and (c')], respectively, of the ENG/MNG bilayer with different angle of incidence.

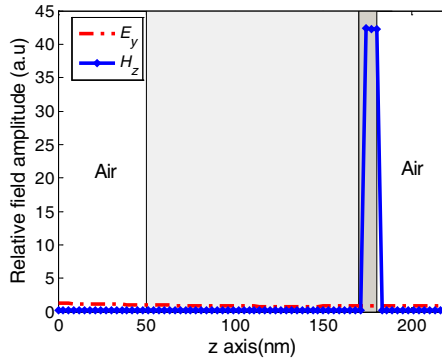


Figure 4. The field distributions in the bilayer structure when the frequency (299.5 THz) is near the reflected valley in Fig. 3(a).

field in the MNG layer is increased by 42 times in comparison with that of incident fields. The physical reason is as follows. For a TE wave, the continuity of the longitudinal component of the magnetic induction field, $B_z = \mu H_z$, at the boundary requires that the value of H_z need a huge jump across the boundary, owing to the sharp contrast of the values of μ in two media when $\mu_{MNG} \rightarrow 0$. The great enhancement of H_z may boost the nonlinear effects if the MNG material has Kerr-type nonlinearity, which facilitates the realization of an optical bistability with low threshold.

3. CONCLUSION

To summarize, we find another type of Fano resonance induced by the special properties at the nihility of dispersive metmaterials, even in a one-dimensional system. Our theoretical analysis shows that the asymmetric Fano-type reflection originates from the coupling between the two different reflection pathways. The variation of the angle of incidence can lead to different Fano asymmetric parameters and different asymmetric Fano resonance spectra. Owing to the simple configuration, some related applications might be explored in this structure in the future.

ACKNOWLEDGMENT

This research was supported by CNKBRFSF (Grant No. 2011CB922001), by NSFC (Grants Nos. 10634050, 11074187 and 51007064), by Shanghai Science and Technology Committee (Grant Nos. 08dj1400301 and 11QA1406900).

REFERENCES

1. Fano, U., "Effects of configuration interaction on intensities and phase shifts," *Phys. Rev.*, Vol. 124, 1866–1878, 1961.
2. Miroshnichenko, A. E., S. Flach, and Y. S. Kivshar, "Fano resonances in nanoscale structures," *Rev. Mod. Phys.*, Vol. 82, 2257–2298, 2010.
3. Kobayashi, K., H. Aikawa, S. Katsumoto, and Y. Iye, "Mesoscopic Fano effect in a quantum dot embedded in an Aharonov-Bohm ring," *Phys. Rev. B*, Vol. 68, 235304, 2003.
4. Vassilios, V. and M. P. Hariton, "Fano resonance and persistent current in mesoscopic open rings: Influence of coupling and Aharonov-Bohm flux," *Phys. Rev. B*, Vol. 74, 235323, 2006.
5. Xiong, Y. J. and X. T. Liang, "Fano resonance and persistent current of a quantum ring," *Phys. Lett. A*, Vol. 330, 307–332, 2004.
6. Fan, S. H., "Sharp asymmetric line shapes in side-coupled waveguide-cavity systems," *Appl. Phys. Lett.*, Vol. 80, 908–910, 2002.
7. Rybin, M. V., A. B. Khanikaev, M. Inoue, A. K. Samusev, M. J. Steel, G. Yushin, and M. F. Limonov, "Bragg scattering induces Fano resonance in photonic crystals," *Photonics and Nanostructures — Fundamentals and Applications*, Vol. 8, 86–93, 2010.
8. Ruan, Z. and S. Fan, "Temporal coupled-mode theory for Fano resonance in light scattering by a single obstacle," *J. Phys. Chem. C*, Vol. 114, 7324–7329, 2009.
9. Chua, S. L., Y. D. Chong, A. D. Stone, M. Solja, and B. A. Jorge, "Low-threshold lasing action in photonic crystal slabs enabled by Fano resonances," *Opt. Express*, Vol. 19, 1540–1562, 2011.
10. Song, J. F., R. P. Zaccaria, M. B. Yu, and X. W. Sun, "Tunable Fano resonance in photonic crystal slabs," *Opt. Express*, Vol. 14, 8812–8826, 2006.
11. Rybin, M. V., A. B. Khanikaev, M. Inoue, K. B. Samusev, M. J. Steel, G. Yushin, and M. F. Limonov, "Fano resonance between Mie and Bragg scattering in photonic crystals," *Phys. Rev. Lett.*, Vol. 103, 023901, 2009.
12. Hao, F., Y. Sonnefraud, P. van Dorpe, S. A. Maier, N. J. Halas, and P. Nordlander, "Symmetry breaking in plasmonic nanocavities: Subradiant LSPR sensing and a tunable Fano resonance," *Nano Lett.*, Vol. 8, 3983–3988, 2008.

13. Luk'yanchuk, B., I. Z. Nikolay, A. M. Stefan, J. H. Naomi, N. Peter, G. Harald, and T. C. Chong, "The Fano resonance in plasmonic nanostructures and metamaterials," *Nature Materials*, Vol. 9, 707–715, 2010.
14. Liu, N., T. Weiss, M. Mesch, and L. Langguth, "Planar metamaterial analogue of electromagnetically induced transparency for plasmonic sensing," *Nano Lett.*, Vol. 10, 1103–1107, 2010.
15. Menzel, C., C. Helgert, C. Rockstuhl, E. Kley, A. Tnnermann, T. Pertsch, and F. Lederer, "Asymmetric transmission of linearly polarized light at optical metamaterials," *Phys. Rev. Lett.*, Vol. 104, 253902, 2010.
16. Pendry, J. B., A. J. Holden, W. J. Stewart, and I. Youngs, "Extremely low frequency plasmons in metallic mesostructures," *Phys. Rev. Lett.*, Vol. 76, 4773–4776, 1996.
17. Zhang, S., W. J. Fan, B. K. Minhas, A. Frauenglass, K. J. Malloy, and S. R. J. Brueck, "Midinfrared resonant magnetic nanostructures exhibiting a negative permeability," *Phys. Rev. Lett.*, Vol. 94, 037402, 2005.
18. Moerland, R. J., N. F. van Hulst, H. Gersen, and L. Kuipers, "Probing the negative permittivity perfect lens at optical frequencies using near-field optics and single molecule detection," *Opt. Express*, Vol. 13, 1604–1614, 2005.
19. Yen, T. J., W. J. Padilla, N. Fang, D. C. Vier, D. R. Smith, J. B. Pendry, D. N. Basov, and X. Zhang, "Terahertz magnetic response from artificial materials," *Science*, Vol. 303, 1494–1496, 2004.
20. Alù, A. and N. Engheta, "Pairing an epsilon-negative slab with a mu-negative slab: Resonance, tunneling and transparency," *IEEE Trans. Antennas Propagat.*, Vol. 51, 2558–2571, 2003.
21. Lin, W. H., C. J. Wu, T. J. Yang, and S. J. Chang, "Analysis of dependence of resonant tunneling on static positive parameters in a single-negative bilayer," *Progress In Electromagnetics Research*, Vol. 118, 151–165, Jan. 2011.
22. Alù, A., M. G. Silveirinha, A. Salandrino, and N. Engheta, "Epsilon-near-zero metamaterials and electromagnetic sources: Tailoring the radiation phase pattern," *Phys. Rev. B*, Vol. 75, 155410, 2007.
23. Yariv, A. and P. Yeh, *Optical Waves in Crystals*, Wiley, New York, 1984.